Article

Poly(tetrasubstituted-aryl imidazole)s: A Way to Obtain Multi-Chromophore Materials with a Tunable Absorption/Emission Wavelength

Edouard Chauveau [1,*], Lara Perrin [2], Catherine Marestin [3] and Régis Mercier [3]

1   Laboratory Charles Coulomb (L2C-UMR5221), University Montpellier, CNRS, Place Eugène Bataillon, 34095 Montpellier, France
2   Laboratory of Electrochemistry and Physicochemistry of Materials and Interfaces (LEPMI-UMR5279), University Grenoble Alpes, University Savoie Mont Blanc, CNRS, Grenoble INP, 38000 Grenoble, France; lara.perrin@univ-smb.fr
3   Laboratory Polymer Materials Engineering (IMP-UMR 5223), University Lyon, University Claude Bernard Lyon 1, CNRS, 15 Boulevard Latarjet, 69622 Villeurbanne, France; catherine.marestin@univ-lyon1.fr (C.M.); regis.mercier@univ-lyon1.fr (R.M.)
*   Correspondence: edouard.chauveau@umontpellier.fr

Abstract: Some original poly(tetrasubstituted imidazole)s incorporating different units were synthesized and characterized. These materials were obtained via a cascade polycondensation process assisted by microwave irradiation that was developed by our team. This time, we integrated two well-known chromophore structures into the macromolecular backbone, which were benzothiadiazole (BTD) and diketopyrrolopyrrole (DKPP). These new polymers were fully characterized: their chemical structures were confirmed using NMR spectroscopy and their thermal, optical and electrochemical properties were investigated and compared with a reference polymer containing a phenyl spacer instead of the mentioned chromophore units. These materials were found to exhibit a large Stokes shift of up to 350 nm. Furthermore, a polymer presenting large absorption on the UV–visible range and an emission close to the near-infrared region was obtained by coupling the mentioned moieties. According to the established properties of this latter polymer, it presents a potential for applications in biological imaging or optoelectronic devices.

Keywords: imidazole; benzothiadiazole; diketopyrrolopyrrole; fluorescent polymers; transfer photoluminescence

1. Introduction

For some time, many new polymers with attractive optical and electronic properties have been regularly synthesized [1–5]. Such polymers with appropriate structures can find several applications and can, for instance, be used in different kinds of sensors like explosive detection devices when possessing turn-on or turn-off fluorescence mechanisms [6,7], or for essential biological component detection or destruction of tumorous cells [8–12]. When prepared as polymer dot nano-particles, polymers can find applications in several areas of interest such as biological imaging and in vivo probes [13]. For biomedical uses, the targeted properties are a high brightness fluorescence in the near-infrared region (NIR), a large Stokes shift or a good Förster resonance energy transfer (FRET) efficiency [14]. To attempt to reach these characteristics, one promising way is the synthesis of poly-chromophore polymers with compatible donor and emitter moieties. That is to say, a good overlap between the donor emission band and the absorption range of the final expected emitter, i.e., the acceptor [15,16].

Fluorescent biological imaging techniques are powerful tools for the non-invasive study of biological mechanisms. In particular, they provide high sensitivity and possess optimal local resolution. Unfortunately, the traditionally used fluorophores are small

organic dyes, which present a restricted photo-stability. It thus seems of interest to develop novel fluorophore materials. Moreover, for in vivo purposes, fluorescence in the near-infrared range is needed due to its high potential for deep tissue penetration [17,18].

The constant development of polymer nanofibers has led to the emergence of a variety of nanofibers with different structural properties, making their use in sensing applications ever more widespread. This allowed the recent development of fluorescence sensors based on polymer nanofibers mixed with fluorescent particles, for instance, the following composites have found applications as optical sensors for the detection of food freshness, pH, mercury ions, gas and volatile organic compounds: cellulose–CdTe quantum dots, polyvinylpyrrolidone–rhodamine, chitosan–carbon dots, polyacrylonitrile–hydroxyphenyl benzoxazole or polyacrylonitrile–small organic dyes [19]. Polymeric microcapsules are also of interest. They can, for instance, contain anticancer drugs and fluorescent nanocrystals for tumor treatment and diagnostics, respectively [20]. Due to their high fluorescence quantum yield, perovskite nanocrystals could also find applications in sensors, for instance, the detection of hazardous materials in food [21]. They should, however, be embedded within a polymeric encapsulation in order to resist environmental stress. Organic dyes have also thoroughly been investigated year after year in order to develop fluorescent probes for various applications, such as biological component detection, bio-imaging and even cancer/tumorous cell therapy. Recent fluorescence probes are mainly based on coumarin, rhodamine, fluorescein, cyanine, boron–dipyrromethene or diketopyrrolopyrrole [12]. Even if diketopyrrolopyrrole evidenced remarkable properties such as superior fluorescence and exceptional photochemical and thermal stability, its development is still immature and needs to be further developed. Its integration in a larger polymeric architecture will therefore be proposed in this manuscript. Indeed, as small organic molecules usually exhibit short emission wavelengths, an interesting strategy could be the redshift of both absorption and emission properties by extension of the conjugated π-system. This is affordable with the oligomerization/polymerization of small conjugated molecules. In this way, Zou et al. produced a benzodithiophene–thiadiazoloquinoxaline alternated oligomer with improved NIR fluorescence [22]. Hernández-Ortiz et al. even highlighted the possibility of obtaining a change in fluorescence emission for the bithiophene–quinolinevinylene alternated polymer [23]. This was possible thanks to a conformational photoisomerization from the trans to the cis isomer of the same polymer, thus shifting the emission from green to orange.

Organic electronics is another large research area that focuses on new macromolecular systems. This field can serve as a source of inspiration in order to select the most promising units to achieve the previously mentioned goals. Indeed, to design more efficient devices (including solar cells, light-emitting diodes, thin film transistors, etc), it was necessary to develop new π-conjugated structures with specific properties. As a first condition, the polymers should have a good thermal resistance to ensure the lifetime of the devices. Aromatic and heterocyclic materials have proved to be a great choice here, further allowing relative ease for tuning semi-conducting properties by incorporating different electron acceptor and donor functional groups [24]. Two well-known acceptor building blocks that were incorporated in both polymers and small molecules for organic electronic applications are benzothiadiazole [25–30] and diketopyrrolopyrrole [31–38]. Both possess electron-withdrawing properties compatible with the aryl imidazole unit selected as donor moiety, as well as attractive luminescent properties [39,40]. On the other hand, several tetrasubstituted aryl imidazole heterocyclic compounds were recently synthesized within our group using a new convenient multicomponent reaction via a cascade polycondensation process assisted by microwave irradiation [41,42]. They possess very high thermal stability and have also demonstrated some promising results as regards their fluorescence and electronic properties [43–48]. The combination through donor/acceptor pairs of all these materials within one polymer will have a determinant effect on its HOMO and LUMO levels, which will undeniably also affect the optical properties. It would therefore be interesting to extend and explore this new family of polymers that are now available to us.

The main weakness of the selected acceptor structures is their poor solubility, which could imply difficulties in polymer synthesis, purification, characterization and final use. Therefore, several works were carried out to increase their solvent processing ability using, for instance, aliphatic side chains or aromatic backbone spacers. These modifications could considerably change the electronic and structural properties of the final polymer [49–51]. In particular, the addition of thiophene spacers will expand the conjugated system and, interestingly, were also proven to increase the emission wavelength in the case of diketopyrrolopyrrole [52]. Another common way to increase polymer solubility is the incorporation of some nitrogen heterocycle structures along the macromolecular backbone, which will be achieved here using the intended aryl imidazole donor units. These latter molecular architectures possess good solubility in common organic solvents [53,54].

According to all the mentioned advantages, we investigated the potential of combining the different moieties within the same polymer. In order to appreciate the effect of each moiety, a series of three polymers were synthesized and characterized. A full analysis was therefore realized with the investigation of absorbance and fluorescence properties, thermal transition and degradation temperatures, together with the determination of energy levels using electrochemistry and a confirmation of the obtained polymers' chemistry through size exclusion chromatography (SEC) and ^{1}H and ^{13}C nuclear magnetic resonance spectroscopy (NMR). The ultimate goal of this conducted work was to combine several chromophores to cover a wide range of the visible spectrum, which was successfully achieved with the polymer P3.

2. Materials and Methods

2.1. Materials

Bis(aryl α-diketone) (M4) is the precursor for the main aryl imidazole repeating unit of all synthesized polymers. It was prepared as described in a previous work [41]. The resulting aryl imidazole unit will be coupled with three different units (M1), (M2) and (M3), which are bis(aryl dialdehyde), benzothiadiazole (BTD) and diketopyrrolopyrrole (DKPP) derivatives, respectively. (M1) was prepared as described in the previous work [41] and the procedure for (M2) and (M3) syntheses is further described in this paper.

Triphenylphosphine, copper iodide and bis(triphenylphosphine)palladium(II) dichloride Pd(PPh$_3$)$_2$Cl$_2$ were purchased from Sigma Aldrich and were used as received. All other reactants and solvents were of reagent grade and also used as received. Microwave-assisted experiments were performed with a Milestone ETHOS microwave oven. The polymerizations were performed in a high-pressure Teflon® reactor equipped with a pressure captor and an optical fiber as thermal sensor. The purification by flash chromatography was performed on an Interchim puriflash® 300 and silica (std 15 μm) cartridge was used.

2.2. Synthesis

2.2.1. General Procedure for the Synthesis of M2 and M3

M2 protocol:

4,7-dibromo-2,1,3-benzothiadiazole (A) (2.5 g, 8.5 mmol) and 4-ethynylbenzaldehyde (2.32 g, 18 mmol) were charged into a three-necked reaction vessel equipped with stirrer, argon inlet and reflux condenser. A mixture of dimethylacetamide (DMAc, 23 mL) and triethylamine (23 mL), then copper iodide (57 mg, 0.3 mmol) and triphenylphosphine (56 mg, 0.2 mmol) were added and the solution was stirred for 15 min. Finally, bis(triphenylphosphine)palladium(II) dichloride (60 mg, 0.085 mmol) was added and the mixture was stirred at 80 °C overnight. The yellow precipitate was filtered and washed with acetone, HCl (0.1 N) and methanol, dried under vacuum at 80 °C to yield 2.6 g of the M2 titled compound (78% yield) as a yellow powder.

4,4′-[2,1,3-benzothiadiazole-4,7-diyldi(ethyne-2,1-diyl)]dibenzaldehyde (M2): (mp: no melting point found before degradation temperature). ^{1}H NMR (500 MHz, CDCl$_3$, 25 °C): δ 7.88 (d, J = 8.3 Hz, 4H; H-Ar), 7.94 (s, 2H; H-Ar), 8.00 (d, J = 8.4 Hz, 4H; H-Ar), 10.00 (s, 2H; CHO). ^{13}C NMR (500 MHz, CDCl$_3$, 25 °C): δ 195.0, 161.8, 161.4, 161.0, 160.6, 153.8,

133.8, 118.4, 97.0, 88.8 ppm. (See Figures S1 and S2 in SI for the visualization of ^{1}H and ^{13}C NMR spectra, respectively).

M3 protocol:

3,6-bis(5-bromothiophen-2-yl)-2,5-bis(dodecyl)pyrrolo [3,4-c]pyrrole-1,4-dione (B) (1.4 g, 1.76 mmol) and 4-ethynylbenzaldehyde (0.47 g, 36 mmol) were charged into a three-necked reaction vessel equipped with stirrer, argon inlet and reflux condenser. A mixture of DMAc (13 mL) and triethylamine (13 mL), then copper iodide (12 mg, 0.06 mmol) and triphenylphosphine (12 mg, 0.04 mmol) were added and the solution was stirred for 15 min. Finally, bis(triphenylphosphine)palladium(II) dichloride (12 mg, 0.02 mmol) was added and the mixture was stirred at 80 °C overnight. The dark blue precipitate was filtered and washed with water, the product was purified by flash chromatography using chloroform as eluent to afford 0.92 g (58% yield) of the M3 titled compound as a dark blue solid.

4-{2-[5-(2,5-bis(dodecyl)-4-{5-[2-(4-formylphenyl)ethynyl]thiophen-2-yl}-3,6-dioxopyrrolo [3,4-c]pyrrol-1-yl)thiophen-2-yl]ethynyl}benzaldehyde (M3): mp = 157 °C. ^{1}H NMR (500 MHz, CDCl$_3$ + trifluoroacetic acid, 25 °C): δ 0.86 (t, J = 6.95 Hz, 6H; CH$_3$), 1.35–1.42 (m, 36H), 1.75 (m, 4H), 4.07 (t, J = 7.80, 4H), 7.50 (d, J = 4.15, 2H), 7.74 (d, J = 8.3, 4H), 7.97(d, J = 8.4, 4H), 8.76 (d, J = 4.15, 2H), 10.00 (s, 2H). ^{13}C NMR (500 MHz, CDCl$_3$ + trifluoroacetic acid, 25 °C): δ 195, 161.8, 161.3, 160.9, 160.5, 160.1, 140.8, 136.5, 134.8, 130.4, 129.3, 108.8, 97.3, 86.4, 42.9, 31.9, 29.8–29.1, 26.7, 22.6, 14.0 ppm. (See Figures S4 and S5 in SI for the visualization of ^{1}H and ^{13}C NMR spectra, respectively).

2.2.2. General Procedure for the Polymerization of P1, P2 and P3

Polymers:

The polymerizations were performed under microwaves (2.45 GHz, 500 W) for 40 min at 140 °C following a procedure already described in our previous work for polymer P1 [42]. The polymers were obtained by precipitation in methanol, filtered and then washed with methanol using a Soxhlet extractor to remove p-buthylaniline and ammonium acetate.

P1 was obtained as off-white colored solid, P2 was obtained as an orange solid and P3 was obtained as a dark blue metallic like solid. All polymers presented a monomodal molecular weight distribution. ^{1}H and ^{13}C NMR spectra of P2 and P3 new polymers are presented in SI (Figures S7–S10) and the typical SEC profile in Figure S11 (molecular weights are given later in the manuscript).

2.3. Characterizations

2.3.1. Chemical Structure Control

Nuclear magnetic resonance (NMR) spectra were recorded on a Bruker Avance 500 MHz spectrometer (Bruker, Preston, VIC, Australia). Deuterated chloroform (CDCl$_3$) was used as solvent, with, if needed, the help of a drop of trifluoroacetic acid (TFA).

The molecular weights of the polymers were measured by size exclusion chromatography (SEC) using a system equipped with a generic pump coupled with a differential refractive index detector (Wyatt optilab-rEX (Waters Corporation, Milford, MA, USA) 25 °C at 658 nm). Molecular weight parameters (Mw, Mn, Đ = Mw/Mn) are given in 'polystyrene equivalent molecular weights' obtained using chloroform as eluent and a calibration with polystyrene standards.

2.3.2. Thermal Analyses

Thermogravimetric analyses (TGA) were performed under nitrogen on a Mettler TGA1 from 25 to 600 °C at 10 °C/min. The polymer glass transition temperatures (Tg) were determined by Differential Scanning Calorimetry (DSC) from a TA instrument Q2000 measurements (TA Instruments, New Castle, DE, USA). Analyses were performed under nitrogen, at a heating rate of 10 °C/min, on a 25–300 °C temperature range. Reported values were obtained from the second heat scan, using the midpoint method.

2.3.3. Optical Properties

Absorption spectra were measured using a Varian Cary50 UV–visible spectrophotometer (Spectralab Scientific Inc., Markham, ON, Canada). Polymer solution photoluminescence spectra (Agilent, Santa Clara, CA, USA) were recorded with an Agilent Cary Eclypse spectrofluorometer. The fluorescence quantum yields were determined using the procedure described by G.A. Crosby and J.N. Demas [55].

2.3.4. Electrochemical Properties

The electrochemical experiments were carried out with a Biologic SP-300 potentiostat (Bio-Logic, Knoxsville, TN, USA). The cyclic voltammetry was performed in a three-electrode cell equipped with platinum working electrode (2.01 mm^2), platinum counter-electrode and Ag/Ag$^+$ reference electrode (silver wire in an acetonitrile solution of AgNO$_3$ (0.01 M) and tetrabutylammonium hexafluorophosphate TBAHFP (0.1 M)). Experiments were conducted in anhydrous and nitrogen-saturated 0.1 M TBAHFP solutions and analyzed compounds were under the form of films (polymer diluted solutions dropped and evaporated on the working electrode). Electrolyte solutions and scan rate conditions used were propylene carbonate at 20 mV·s^{-1}. The reference electrode was calibrated versus the ferrocene/ferrocenium couple (Fc/Fc$^+$) measured under the form of solution in same experimental conditions. As the potential of Ag/Ag$^+$ reference electrode can vary between experiments due to the possible little evolution of [Ag$^+$], presented potentials are referenced to an external reference compound with a known $E_{\frac{1}{2}}$, which was measured and verified to be constant before and after all measurements campaigns (measured $E_{1/2}$(Fc/Fc$^+$) = 0.08 V vs. Ag/AgCl). Reported oxidation and reduction potentials for polymers are the onset potentials determined using the tangent method.
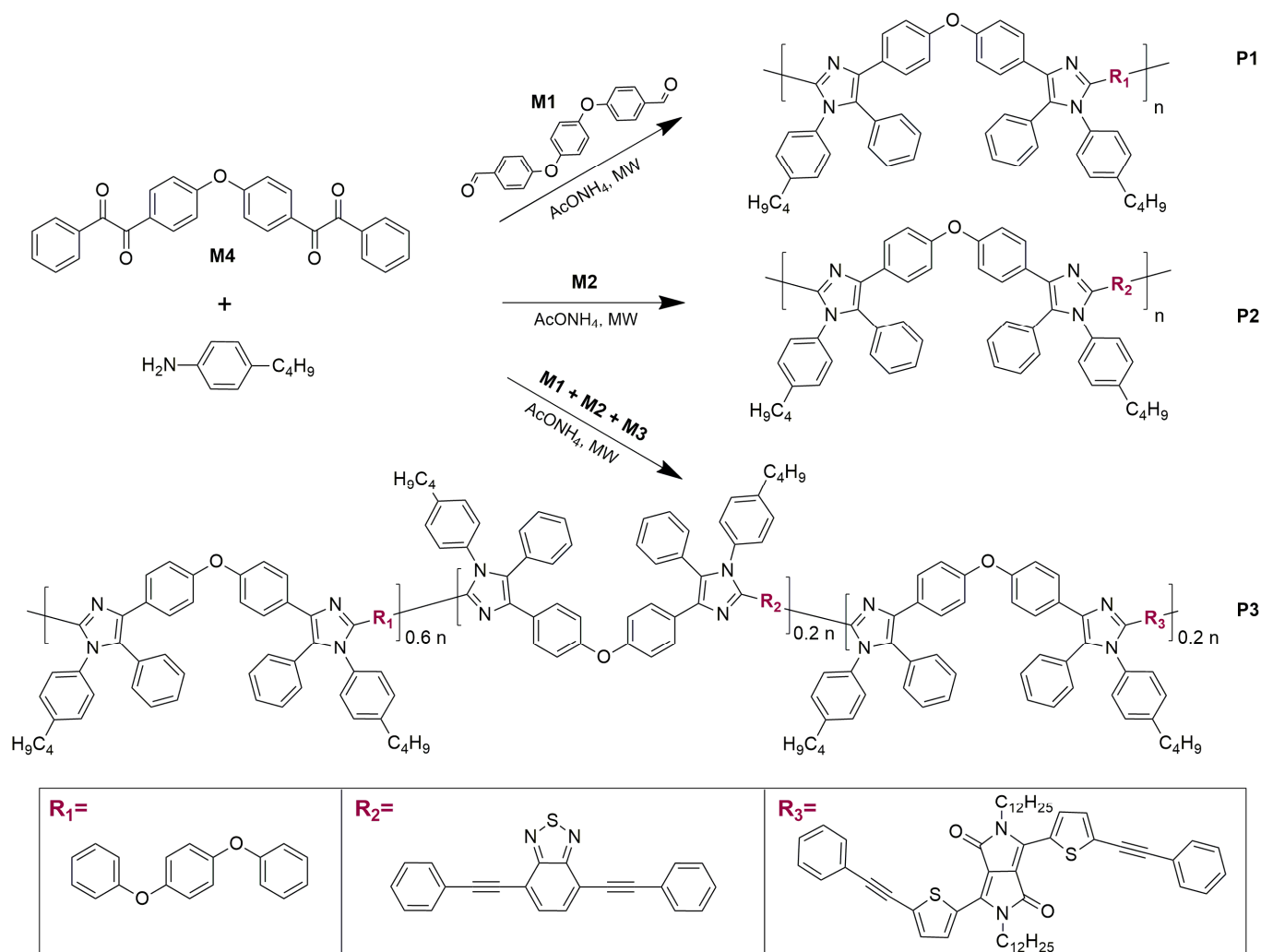
3. Results and Discussions

In order to successfully synthesize the poly(tetrasubstituted imidazole) copolymer series, the chosen experimental conditions involve bis(arylaldehyde) and bis(aryl α-diketone) compounds in stoichiometric ratio [42]. While the reference polymer P1 was synthetized using the previously developed (phenylene bis(oxy))dibenzaldehyde (M1), it was thus necessary to functionalize both selected chromophore units to afford P2 and P3. Scheme 1 thus presents the synthetic pathway to obtain the two required monomers M2 and M3, which are the benzothiadiazole and diketopyrrolopyrrole derivatives, respectively. Intermediates A and B were synthesized according to the reported procedures [35,56,57], following the steps that can be found in Scheme S1 presented in the Supporting Information file.
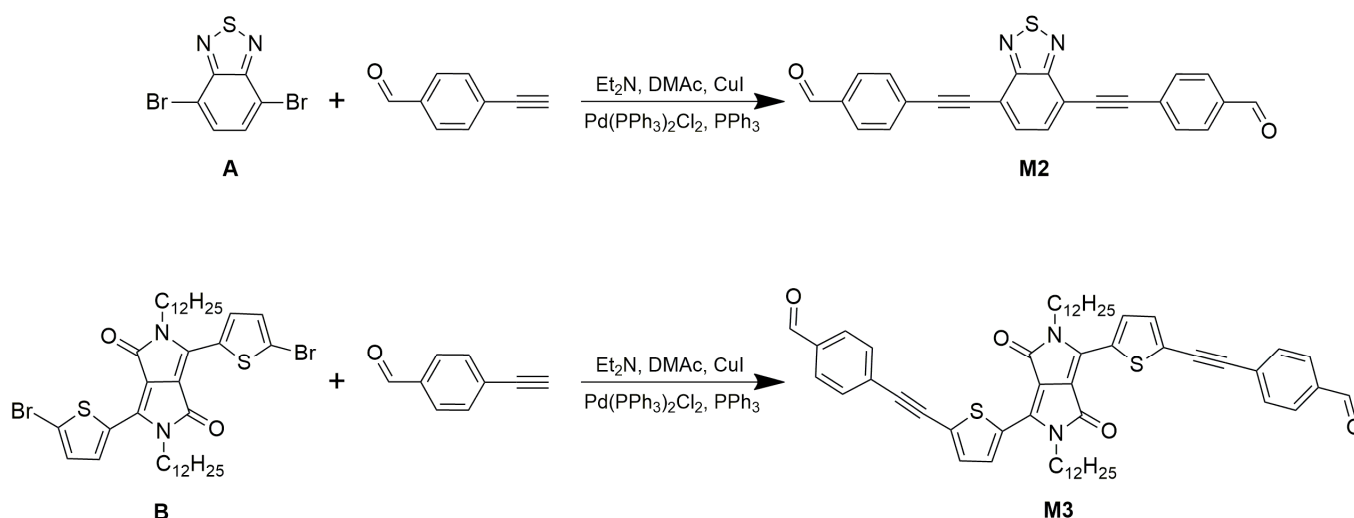
Scheme 1. Synthetic route to the dialdehyde monomers M2 and M3.

The described final step to reach the dialdehyde monomers consists of a Sonogashira coupling reaction involving the dibrominated intermediates and the acetylenic benzaldehyde. The use of a mixture of triethylamine and dimethylacetamide (DMAc), in the presence of the catalytic system comprising triphenylphosphine, copper iodide and $PdCl_2(PPh_3)_2$, provides a good yield and an easy workup. P1, P2 and P3 were then obtained as described in Scheme 2: M1, M2 and M3 were allowed to react with M4 into a one-pot polycondensation with ammonium acetate and 4-butylaniline to furnish the polymers P1, P2 and P3 as consistent materials.
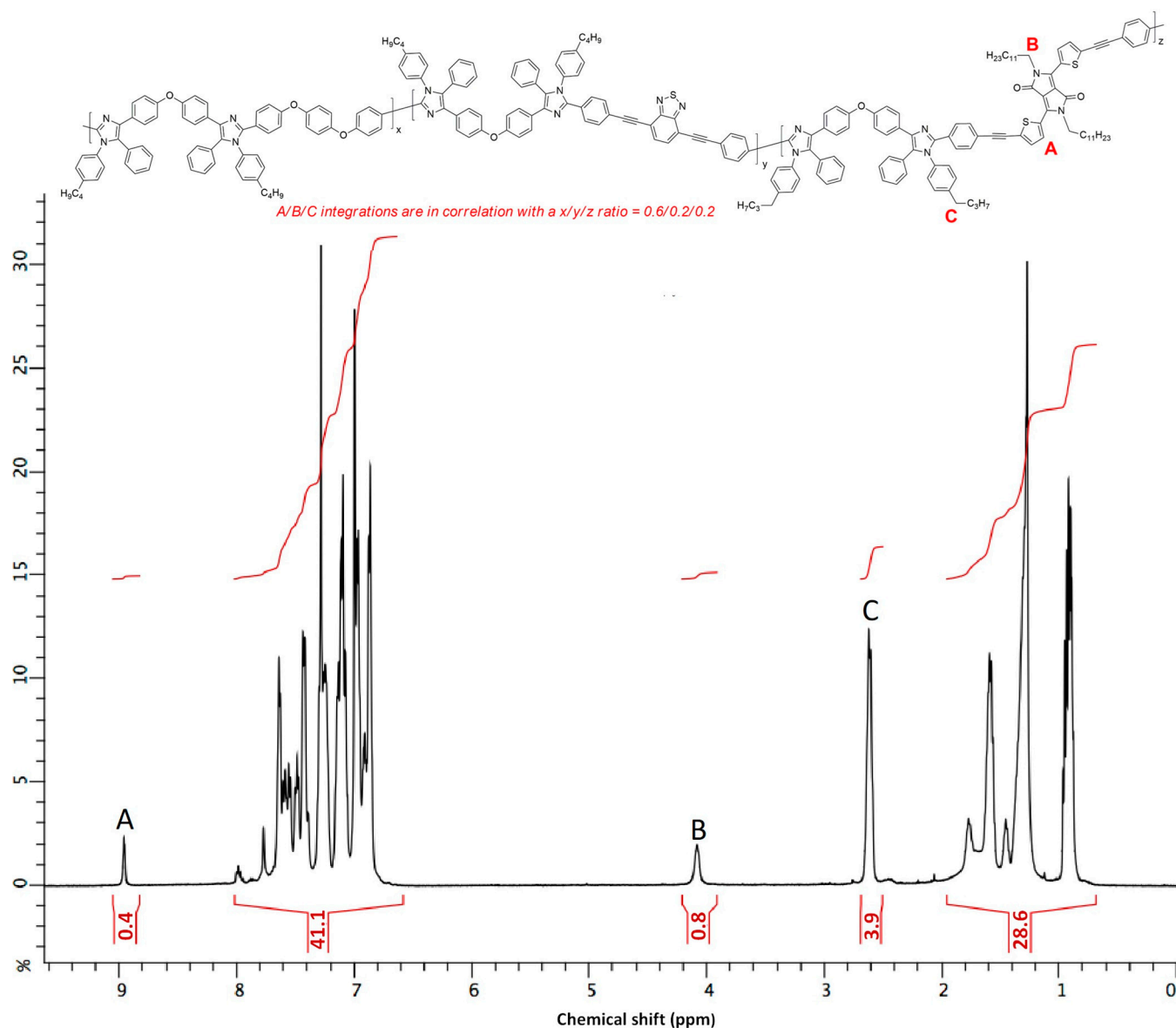

Scheme 2. Synthetic pathway for polymers P1, P2 and P3.

These poly(tetraaryl imidazoles) (PTAI) copolymers were synthesized using the Debus–Radziszewski reaction under microwave irradiation. This technique is useful to quickly and easily access some new macromolecular structures [58,59]. The chemical structure of newcomer's polymers P2 and P3 were checked using ^{1}H and ^{13}C NMR (see SI for all spectra). The following Figure 1 presents as example of the ^{1}H NMR spectrum of polymer P3. This polymer was completely soluble in chloroform, providing a solution with low viscosity. The incorporation of the DKPP monomer into the polymer backbone was evidenced by the presence of characteristic peaks: C-H (A) from the thiophene rings and N-CH$_2$ (B) from the alkyl chains. In addition, the Ar-CH$_2$ (C) signal attributed to the butylaniline chemical group (belonging to the aryl imidazole units) shows a good correlation with the expected ratios for M1-, M2- and M3-based repeating units (i.e., 0.6/0.2/0.2), respectively, corresponding to all the components initially engaged in the polymerization.

Figure 1. ^{1}H NMR spectrum of polymer P3 at 25 °C in CDCl$_3$ (the integration around 7 ppm could be distorted by residual CHCl$_3$ in CDCl$_3$).

The molecular weights of all the polymers were high enough to make self-supporting thin films using the classical solvent evaporation process, as shown in Figure 2 and confirmed by the SEC values reported in Table 1.


Figure 2. Thin films of polymers P1, P2 and P3 under (**a**) natural light and (**b**) UV-365 nm irradiation.

Table 1. Thermal properties and molecular weights of synthetized copolymers.

Polymer	Td $_{5\%}$ (°C) [a]	Tg (°C) [b]	Mn (g·mol^{-1}) [c]	Mw (g·mol^{-1}) [c]	Đ [c]
P1	465	185	31,000	89,000	2.9
P2	450	NO *	29,000	107,000	3.6
P3	445	178	28,000	200,000	7.1

[a] Td $_{5\%}$ is the decomposition temperature at 5% weight lost. [b] Tg is the glass transition temperature at the midpoint method. [c] Mn is the number average molecular weight, Mw the weight average molecular weight and Đ the polydispersity index (=Mw/Mn). * NO: no Tg visible by DSC.

The thermal properties of the synthetized polymers were investigated using DSC and TGA. The obtained traces are shown in Figure 3a,b, respectively. Data summarized in Table 1 show that all materials possess a high thermal stability with a decomposition temperature near 450 °C. P1 and P3 have a glass transition at around 180 °C. For P2, no glass transition could be observed using the DSC technique, which is common with the benzothiadiazole copolymer family [51,60]. For all the polymers, no melting and crystallization peaks were observed. However, the backbone structure rigidity can lead to melting temperatures above degradation. Despite this relative rigid molecular structure, the synthetized materials still have a very good solubility in common organic solvents.
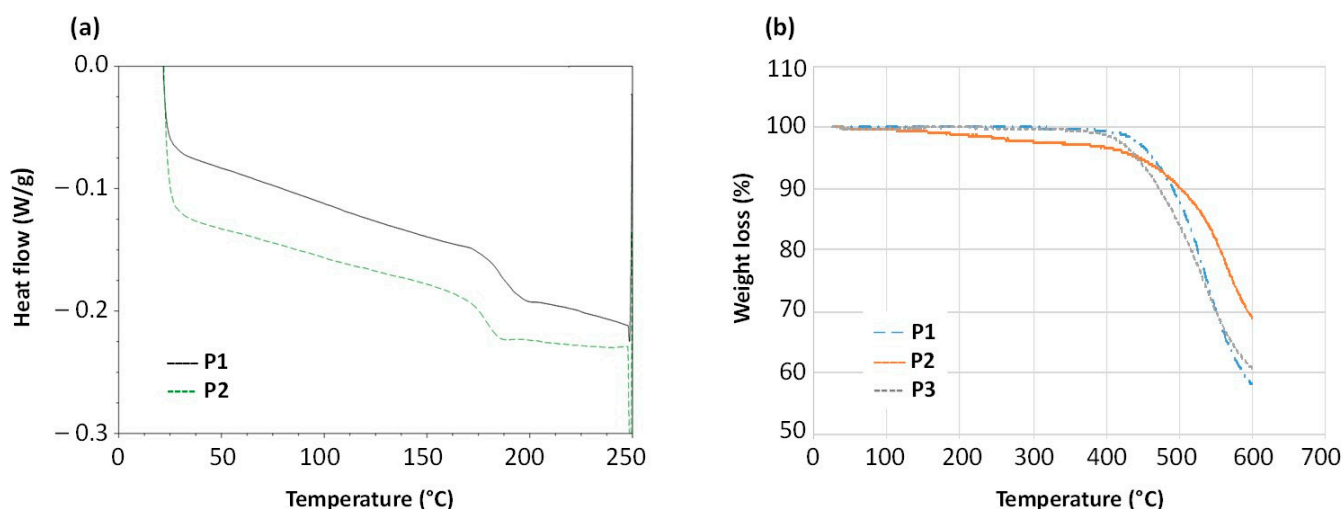
Figure 3. (**a**) DSC and (**b**) TGA traces obtained for synthetized polymers.

In this work, we focused our attention on the incorporation of some well-known chromophores such as benzothiadiazole and diketopyrrolopyrrole structures into the polymer backbone, and the focal point of the present work concerns the investigation of the resulting optical properties. These molecular patterns are widely used in solar cells and other organic electronic devices. However, here, we study them in another kind of "push–pull" structure using a non-common imidazole linkage. The push–pull design is provided by the imidazole as a donor while the benzothiadiazole and diketopyrrolopyrrole units both play the role of electron acceptors. Here, two different and isolated push–pull systems are theoretically present in the polymer P3. This was confirmed by its UV–visible absorption spectrum (Figure 4a), which covers each different copolymer fragment absorptions, the latter being slightly redshifted when compared to those of the monomer units (see Figures S3 and S6 in SI). On another note, the absorbance spectra of polymers P1, P2 and P3 in the solid state were quite close to their equivalents in the solution state; however, a redshift of about 20 nm was witnessed, which is commonly observed due to stacking in the solid state (see Figure S12).
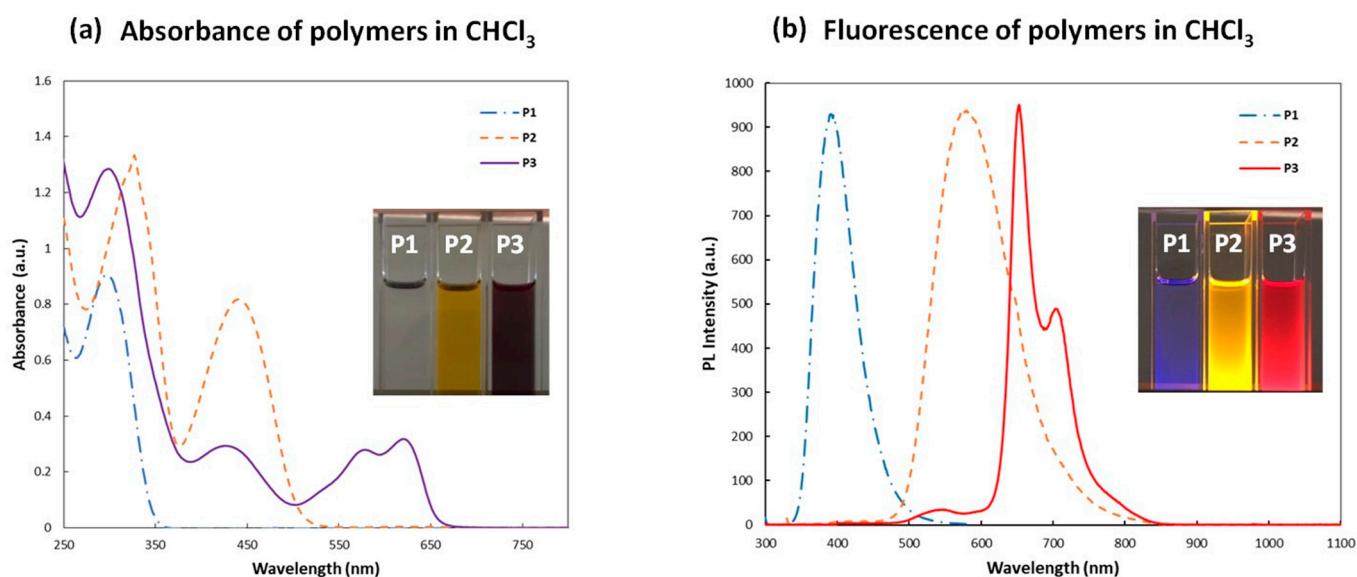
Figure 4. Absorption (**a**) and emission (**b**) spectra of the polymers in CHCl$_3$ solution.

As regards the luminescence properties of the synthetized polymers, all possess luminescent properties in the solution state (Figure 3b), but only P1 and P2 exhibited a signal in the solid state (Figure 2b). This should originate from a strong π–π aggregation of the diketopyrrolopyrrole units [61], inducing a strong fluorescence quenching in the solid state for P3. Interestingly, according to the liquid state photoluminescence spectra (Figure 4b), we can observe a kind of FRET transfer with polymers P2 and P3 that affords a large Stokes shift of up to 350 nm (λex = maximum of λabs reported in Table 2). The fluorescence contribution of the BTD moiety at about 550 nm was estimated to be less than 0.2% in polymer P3 and, as expected, the incorporation of the DKPP structure affords a maximum fluorescence emission between 650 and 700 nm (the latter being in accordance with the monomer unit fluorescence, see Figures S3 and S6 in SI). It could be observed that both the absorption and emission patterns of the DKPP moiety consist of two peaks. This is the case for both the polymer P3 and its corresponding monomer unit M3 (see Figure S6 in SI). According to the literature [62], the two clear vibronic peaks correspond to the 0–1 and 0–0 transitions of DKPP, respectively.

Table 2. Optical characterizations (for Mod: model compound, see the SI).

Structure	λabs (nm) (ε.10^3) [a]	λem (nm) [b]	E_g^{opt} (eV) [c]	φ (%) [d]
P1	296 (43)	394	3.5	4
P2	327 (66); 441 (40)	579	2.3	23
P3	297 (50); 430 (5.5); 620 (6)	652–704	1.7	28
Mod	290 (15)	384	3.6	5

[a] λabs: wavelength of the maximum absorption and ε: absorption coefficient. [b] λem: wavelength of the maximum emission. [c] E_g^{opt}: optical band gap. [d] φ: fluorescence quantum yield.

Table 2 presents the absorption and emission wavelengths at maximal intensities for the three synthesized polymers, together with the optical bandgap (E_g^{opt}) values decreasing from 3.5 eV to 1.7 eV when passing from polymer P1 to polymer P3. The polymers' fluorescence quantum yields were also determined and totaled up to about 25–30% for polymers P2 and P3 (Table 2). These values are near the literature data for molecules or polymers based on similar units [38,46], but it should be observed that polymer P1 presents a very low fluorescence yield. This should be due to the n-π* excitation state, which is a relative long lifetime radiation process that induces a low quantum yield of the single

state fluorescence [63]. To confirm this result originating from the imidazole core, a small tetraaryl imidazole model molecule (Mod) was synthesized (see the SI for its synthesis and characterization: Scheme S2 and Figures S13–S16). The recorded absorbance and fluorescence emission spectra permit us to calculate the fluorescence quantum yield of this model molecule, which was found to be in the same range as that of polymer P1, i.e., about 5%. This means that the higher fluorescence yields found for P2 and P3 are due to the molecular structures of the BTD and DKPP moieties.

On the other hand, a very good overlap was evidenced between the emission wavelengths of the P1 and P2 emitters and the absorption of the DKPP acceptor. If we consider that the DKPP is only present in 20% of P3 repeating units, the yield of fluorescence using FRET processing is thus very good.

In order to go further and estimate the energy levels of this new copolymer series, an electrochemical study was conducted. Figure 5 presents the cyclic voltammograms (CV) obtained for the three polymers. Concerning positive potentials, all polymers present one irreversible oxidation peak with close values. The switching between the different acceptor units demonstrated no significant impact on the associated HOMO levels (see Table 3). Indeed, the observed oxidation answer is attributed to the shared imidazole donor moiety.
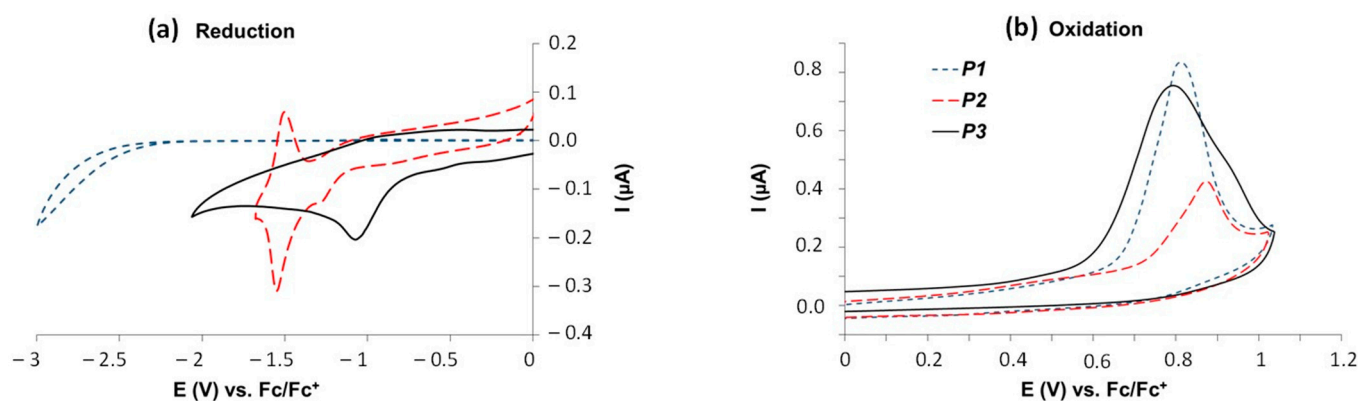

Figure 5. Cyclic voltammograms of polymers P1, P2 and P3.

Table 3. Electrochemical data and HOMO/LUMO levels of polymers.

Polymer	E^{OX}_{onset} (V) [a] vs. Fc/Fc$^+$	E^{RED}_{onset} (V) [a] vs. Fc/Fc$^+$	HOMO [b] (IP, eV)	LUMO [b] (EA, eV)	E^{CV}_g (eV) [d]
P1	0.67	-	−5.8	∼−2.3 [c]	-
P2	0.73	−1.35	−5.8	−3.8	2.08
P3	0.61	−0.82	−5.7	−4.3	1.43

[a] E^{OX}_{onset} and E^{RED}_{onset} are, respectively, the first onset oxidation and reduction potentials determined by CV and are given versus the ferrocene/ferrocenium standard couple. [b] Except in c case, the HOMO and LUMO values were calculated with respect to ferrocene (reference energy level = −5.1 eV below the vacuum level) according to the following equations: HOMO = −[(E^{OX}_{onset} vs. Fc/Fc$^+$) + 5.1]; LUMO = −[(E^{RED}_{onset} vs. Fc/Fc$^+$) + 5.1]. [c] In this case, the LUMO level was estimated using E^{opt}_g. [d] E^{CV}_g: electrochemical band gap.

Regarding the negative potentials, reduction waves were observed for only two derivatives. For P1, the optical band gap value (given in Table 2 and determined using the UV–visible absorption onset [64]) leads us to think that the reduction peak should take place after −2.5 V. Due to the solvent front (beginning at ∼−2.2 V for propylene carbonate), it seems obvious that this polymer reduction cannot be observed using CV. The obtained curve is, however, shown in Figure 5 (intensity values in ordinate were divided by ten in order to be presented on the same graph as P2 and P3 voltammograms), and nothing was detectable except the solvent breakdown. Consequently, the optical band gap was used

to estimate the P1 polymer's LUMO value. Respectively, for P2 and P3, a quasi-reversible reduction peak at -1.35 V and an irreversible peak at -0.82 V vs. Fc/Fc$^+$ were observed, demonstrating both electrochemical band gaps in accordance with optical ones. The three resulting LUMO levels (Table 3) are mainly controlled by the LUMO level of the polymers acceptor moieties and thus driven by the increasing electron-withdrawing strength of the following units: diphenyl ether < benzothiadiazole < diketopyrrolopyrrole.

It should be observed that for polymer P3, no second reduction wave was observed at benzothiadiazole potential, even though this unit is present in the same quantity as the diketopyrrolopyrrole unit. This might be related to an intramolecular decomposition due to the first irreversible reduction and not reproducible using cycling.

4. Conclusions

New polychromophore materials were successfully synthesized using an innovative multi-component polycondensation. These macromolecules have several interesting properties such as good thermal stability and high solubility. We demonstrated that it was possible to tune their optical characteristics by changing the di-aryl aldehyde functionalized monomer, which is a relatively easily accessible modification. In this work, we succeeded in affording a polymer with a large Stoke shift of about 350 nm. This polymer family could probably have several interesting applications in both biological imaging or optoelectronic devices, and it seems of interest to investigate possible adjustments on the donor moiety, i.e., the imidazole ring that is governed by the α-diketone monomer.

Supplementary Materials: The following supporting information can be downloaded at: https://www.mdpi.com/article/10.3390/pr11102959/s1, Figure S1: ^{1}H NMR spectrum of monomer M2 in CDCl$_3$, Figure S2: ^{13}C NMR spectrum of monomer M2 in CDCl$_3$, Figure S3: Excitation and emission spectra of monomer M2 in CHCl$_3$, Figure S4: ^{1}H NMR spectrum of monomer M3 in CDCl$_3$ +TFA, Figure S5: ^{13}C NMR spectrum of monomer M3 in CDCl$_3$ + TFA, Figure S6: Excitation and emission spectra of monomer M3 in CHCl$_3$, Figure S7: ^{1}H NMR spectrum of polymer P2 in CDCl$_3$, Figure S8: ^{13}C NMR spectrum of polymer P2 in CDCl$_3$, Figure S9: ^{1}H NMR spectrum of polymer P3 in CDCl$_3$, Figure S10: ^{13}C NMR spectrum of polymer P3 in CDCl$_3$, Figure S11: Typical SEC trace (P3), Figure S12: UV–Vis absorbance spectra of P1, P2 and P3 (in solid state), Figure S13: ^{1}H NMR spectrum of model compound Mod in CDCl3, Figure S14: ^{13}C NMR spectrum of model compound Mod in CDCl$_3$, Figure S15: Absorbance spectrum of the model compound Mod in CHCl$_3$, Figure S16: Excitation (left) and emission (right) spectra of the model compound Mod in CHCl$_3$, Scheme S1: Synthetic route to A and B compounds, chemical building blocks for monomers M2 and M3, Scheme S2: Synthetic route for tetra-aryl imidazole model molecule (Mod), according to a procedure described by K. Pradhan et al.

Author Contributions: Conceptualization, E.C., L.P., C.M. and R.M.; methodology, E.C.; investigation, E.C. and L.P.; writing—original draft preparation, E.C.; writing—review and editing, E.C., L.P., C.M. and R.M. All authors have read and agreed to the published version of the manuscript.

Data Availability Statement: The data presented in this study are available on request from the corresponding author.

Conflicts of Interest: The authors declare no conflict of interest.

References

1. Qi, Y.; Li, N.; Xia, X.; Ge, J.; Lu, J.; Xu, Q. Synthesis of a Fluorescent Chemosensor Based on a New Copolymer Containing Multi-Fluorophore. *Mater. Chem. Phys.* **2010**, *124*, 726–731. [CrossRef]
2. Tang, X.; Zheng, C.; Chen, Y.; Zhao, Z.; Qin, A.; Hu, R.; Tang, B.Z. Multicomponent Tandem Polymerizations of Aromatic Diynes, Terephthaloyl Chloride, and Hydrazines toward Functional Conjugated Polypyrazoles. *Macromolecules* **2016**, *49*, 9291–9300. [CrossRef]

3. Wei, B.; Li, W.; Zhao, Z.; Qin, A.; Hu, R.; Tang, B.Z. Metal-Free Multicomponent Tandem Polymerizations of Alkynes, Amines, and Formaldehyde toward Structure- and Sequence-Controlled Luminescent Polyheterocycles. *J. Am. Chem. Soc.* **2017**, *139*, 5075–5084. [CrossRef]

4. Rekaï, E.D.; Baudin, J.-B.; Jullien, L.; Ledoux, I.; Zyss, J.; Blanchard-Desce, M. A Hyperpolar, Multichromophoric Cyclodextrin Derivative: Synthesis, and Linear and Nonlinear Optical Properties. *Chem. A Eur. J.* **2001**, *7*, 4395–4402. [CrossRef]

5. Schwartz, E.; Le Gac, S.; Cornelissen, J.J.L.M.; Nolte, R.J.M.; Rowan, A.E. Macromolecular Multi-Chromophoric Scaffolding. *Chem. Soc. Rev.* **2010**, *39*, 1576–1599. [CrossRef] [PubMed]

6. Bondarchuk, S. V Theoretical Study of the Meisenheimer and Charge-Transfer Complexes Formed upon Colorimetric Determination of Nitroaromatic Explosives. *FirePhysChem* **2023**, *3*, 164–172. [CrossRef]

7. Enlow, M.A. Binding of TNT to Amplifying Fluorescent Polymers: An Ab Initio and Molecular Dynamics Study. *J. Mol. Graph. Model.* **2012**, *33*, 12–18. [CrossRef] [PubMed]

8. Abelha, T.F.; Morris, G.; Lima, S.M.; Andrade, L.H.C.; McLean, A.J.; Alexander, C.; Calvo-Castro, J.; McHugh, C.J. Development of a Neutral Diketopyrrolopyrrole Phosphine Oxide for the Selective Bioimaging of Mitochondria at the Nanomolar Level. *Chem. A Eur. J.* **2020**, *26*, 3173–3180. [CrossRef] [PubMed]

9. Chiminazzo, A.; Borsato, G.; Favero, A.; Fabbro, C.; McKenna, C.E.; Dalle Carbonare, L.G.; Valenti, M.T.; Fabris, F.; Scarso, A. Diketopyrrolopyrrole Bis-Phosphonate Conjugate: A New Fluorescent Probe for In Vitro Bone Imaging. *Chem. A Eur. J.* **2019**, *25*, 3617–3626. [CrossRef]

10. Ghosh, S.; Shankar, S.; Philips, D.S.; Ajayaghosh, A. Diketopyrrolopyrrole-Based Functional Supramolecular Polymers: Next-Generation Materials for Optoelectronic Applications. *Mater. Today Chem.* **2020**, *16*, 100242. [CrossRef]

11. Wang, Q.; Xia, B.; Xu, J.; Niu, X.; Cai, J.; Shen, Q.; Wang, W.; Huang, W.; Fan, Q. Biocompatible Small Organic Molecule Phototheranostics for NIR-II Fluorescence/Photoacoustic Imaging and Simultaneous Photodynamic/Photothermal Combination Therapy. *Mater. Chem. Front.* **2019**, *3*, 650–655. [CrossRef]

12. Auwalu, M.A.; Cheng, S. Diketopyrrolopyrrole Fluorescent Probes, Photophysical and Biological Applications. *Chemosensors* **2021**, *9*, 44. [CrossRef]

13. Chen, D.; Wu, I.-C.; Liu, Z.; Tang, Y.; Chen, H.; Yu, J.; Wu, C.; Chiu, D.T. Semiconducting Polymer Dots with Bright Narrow-Band Emission at 800 Nm for Biological Applications. *Chem. Sci.* **2017**, *8*, 3390–3398. [CrossRef] [PubMed]

14. Zhang, Y.; Autry, S.A.; McNamara, L.E.; Nguyen, S.T.; Le, N.; Brogdon, P.; Watkins, D.L.; Hammer, N.I.; Delcamp, J.H. Near-Infrared Fluorescent Thienothiadiazole Dyes with Large Stokes Shifts and High Photostability. *J. Org. Chem.* **2017**, *82*, 5597–5606. [CrossRef] [PubMed]

15. Zhang, D.; Zhu, M.; Zhao, L.; Zhang, J.; Wang, K.; Qi, D.; Zhou, Y.; Bian, Y.; Jiang, J. Ratiometric Fluorescent Detection of Pb2+ by FRET-Based Phthalocyanine-Porphyrin Dyads. *Inorg. Chem.* **2017**, *56*, 14533–14539. [CrossRef] [PubMed]

16. Dryza, V.; Smith, T.A.; Bieske, E.J. Blue to Near-IR Energy Transfer Cascade within a Dye-Doped Polymer Matrix, Mediated by a Photochromic Molecular Switch. *Phys. Chem. Chem. Phys.* **2016**, *18*, 5095–5098. [CrossRef]

17. Ding, C.; Ren, T. Near Infrared Fluorescent Probes for Detecting and Imaging Active Small Molecules. *Coord. Chem. Rev.* **2023**, *482*, 215080. [CrossRef]

18. Chen, Y.; Wang, S.; Zhang, F. Near-Infrared Luminescence High-Contrast in Vivo Biomedical Imaging. *Nat. Rev. Bioeng.* **2023**, *1*, 60–78. [CrossRef]

19. Li, J.; Liu, X.; Xi, J.; Deng, L.; Yang, Y.; Li, X.; Sun, H. Recent Development of Polymer Nanofibers in the Field of Optical Sensing. *Polymers* **2023**, *15*, 3616. [CrossRef] [PubMed]

20. Navolokin, N.; Lomova, M.; Bucharskaya, A.; Godage, O.; Polukonova, N.; Shirokov, A.; Grinev, V.; Maslyakova, G. Antitumor Effects of Microencapsulated Gratiola Officinalis Extract on Breast Carcinoma and Human Cervical Cancer Cells In Vitro. *Materials* **2023**, *16*, 1470. [CrossRef] [PubMed]

21. Zhao, W.; Zhang, J.; Kong, F.; Ye, T. Application of Perovskite Nanocrystals as Fluorescent Probes in the Detection of Agriculture- and Food-Related Hazardous Substances. *Polymers* **2023**, *15*, 2873. [CrossRef]

22. Zou, T.; Liu, Y.; Zhang, X.; Chen, L.; Xu, Q.; Ding, Y.; Li, P.; Xie, C.; Yin, C.; Fan, Q. Oligomerization Strategy of D-A-Type Conjugated Molecules for Improved NIR-II Fluorescence Imaging. *Polymers* **2023**, *15*, 3451. [CrossRef] [PubMed]

23. Hernández-Ortiz, O.J.; Castro-Monter, D.; Rodríguez Lugo, V.; Moggio, I.; Arias, E.; Reyes-Valderrama, M.I.; Veloz-Rodríguez, M.A.; Vázquez-García, R.A. Synthesis and Study of the Optical Properties of a Conjugated Polymer with Configurational Isomerism for Optoelectronics. *Materials* **2023**, *16*, 2903. [CrossRef] [PubMed]

24. Beaupré, S.; Shaker-Sepasgozar, S.; Najari, A.; Leclerc, M. Random D–A1–D–A2 Terpolymers Based on Benzodithiophene, Thiadiazole[3,4-e]Isoindole-5,7-Dione and Thieno[3,4-c]Pyrrole-4,6-Dione for Efficient Polymer Solar Cells. *J. Mater. Chem. A* **2017**, *5*, 6638–6647. [CrossRef]

25. DaSilveira Neto, B.A.; Lopes, A.S.; Ebeling, G.; Gonçalves, R.S.; Costa, V.E.U.; Quina, F.H.; Dupont, J. Photophysical and Electrochemical Properties of π-Extended Molecular 2,1,3-Benzothiadiazoles. *Tetrahedron* **2005**, *61*, 10975–10982. [CrossRef]

26. Blouin, N.; Michaud, A.; Leclerc, M. A Low-Bandgap Poly(2,7-Carbazole) Derivative for Use in High-Performance Solar Cells. *Adv. Mater.* **2007**, *19*, 2295–2300. [CrossRef]

27. Chen, C.-H.; Hsieh, C.-H.; Dubosc, M.; Cheng, Y.-J.; Hsu, C.-S. Synthesis and Characterization of Bridged Bithiophene-Based Conjugated Polymers for Photovoltaic Applications: Acceptor Strength and Ternary Blends. *Macromolecules* **2010**, *43*, 697–708. [CrossRef]

28. Horie, M.; Majewski, L.A.; Fearn, M.J.; Yu, C.-Y.; Luo, Y.; Song, A.; Saunders, B.R.; Turner, M.L. Cyclopentadithiophene Based Polymers—A Comparison of Optical, Electrochemical and Organic Field-Effect Transistor Characteristics. *J. Mater. Chem.* **2010**, *20*, 4347–4355. [CrossRef]

29. Rudenko, A.E.; Wiley, C.A.; Stone, S.M.; Tannaci, J.F.; Thompson, B.C. Semi-Random P3HT Analogs via Direct Arylation Polymerization. *J. Polym. Sci. Part A Polym. Chem.* **2012**, *50*, 3691–3697. [CrossRef]

30. Ko, S.; Mondal, R.; Risko, C.; Lee, J.K.; Hong, S.; McGehee, M.D.; Brédas, J.-L.; Bao, Z. Tuning the Optoelectronic Properties of Vinylene-Linked Donor−Acceptor Copolymers for Organic Photovoltaics. *Macromolecules* **2010**, *43*, 6685–6698. [CrossRef]

31. Duvva, N.; Raptis, D.; Kumar, C.V.; Koukaras, E.N.; Giribabu, L.; Lianos, P. Design of Diketopyrrolopyrrole Chromophores Applicable as Sensitizers in Dye-Sensitized Photovoltaic Windows for Green Houses. *Dye. Pigment.* **2016**, *134*, 472–479. [CrossRef]

32. Li, W.; Hendriks, K.H.; Wienk, M.M.; Janssen, R.A.J. Diketopyrrolopyrrole Polymers for Organic Solar Cells. *Acc. Chem. Res.* **2016**, *49*, 78–85. [CrossRef] [PubMed]

33. Grzybowski, M.; Gryko, D.T. Diketopyrrolopyrroles: Synthesis, Reactivity, and Optical Properties. *Adv. Opt. Mater.* **2015**, *3*, 280–320. [CrossRef]

34. Li, Y.; Sonar, P.; Murphy, L.; Hong, W. High Mobility Diketopyrrolopyrrole (DPP)-Based Organic Semiconductor Materials for Organic Thin Film Transistors and Photovoltaics. *Energy Environ. Sci.* **2013**, *6*, 1684–1710. [CrossRef]

35. Zou, Y.; Gendron, D.; Badrou-Aïch, R.; Najari, A.; Tao, Y.; Leclerc, M. A High-Mobility Low-Bandgap Poly(2,7-Carbazole) Derivative for Photovoltaic Applications. *Macromolecules* **2009**, *42*, 2891–2894. [CrossRef]

36. Sonar, P.; Singh, S.P.; Li, Y.; Soh, M.S.; Dodabalapur, A. A Low-Bandgap Diketopyrrolopyrrole-Benzothiadiazole-Based Copolymer for High-Mobility Ambipolar Organic Thin-Film Transistors. *Adv. Mater.* **2010**, *22*, 5409–5413. [CrossRef] [PubMed]

37. Bura, T.; Beaupré, S.; Ibraikulov, O.A.; Légaré, M.-A.; Quinn, J.; Lévêque, P.; Heiser, T.; Li, Y.; Leclerc, N.; Leclerc, M. New Fluorinated Dithienyldiketopyrrolopyrrole Monomers and Polymers for Organic Electronics. *Macromolecules* **2017**, *50*, 7080–7090. [CrossRef]

38. Tieke, B.; Rabindranath, A.R.; Zhang, K.; Zhu, Y. Conjugated Polymers Containing Diketopyrrolopyrrole Units in the Main Chain. *Beilstein J. Org. Chem.* **2010**, *6*, 830–845. [CrossRef]

39. Neto, B.A.D.; Carvalho, P.H.P.R.; Correa, J.R. Benzothiadiazole Derivatives as Fluorescence Imaging Probes: Beyond Classical Scaffolds. *Acc. Chem. Res.* **2015**, *48*, 1560–1569. [CrossRef] [PubMed]

40. Du, C.; Fu, S.; Wang, X.; Sedgwick, A.C.; Zhen, W.; Li, M.; Li, X.; Zhou, J.; Wang, Z.; Wang, H.; et al. Diketopyrrolopyrrole-Based Fluorescence Probes for the Imaging of Lysosomal Zn^{2+} and Identification of Prostate Cancer in Human Tissue. *Chem. Sci.* **2019**, *10*, 5699–5704. [CrossRef]

41. Chauveau, E.; Marestin, C.; Martin, V.; Mercier, R. Microwave-Assisted Polymerization Process: A Way to Design New, High Molecular Weight Poly(Arylimidazole)S. *Polymer (Guildf)* **2008**, *49*, 5209–5214. [CrossRef]

42. Chauveau, E.; Marestin, C.; Mercier, R. Microwave-Assisted Synthesis of Tetrasubstituted Aryl Imidazole Based Polymers via Cascade Polycondensation Process. *Polymer (Guildf)* **2014**, *55*, 6435–6438. [CrossRef]

43. Bae, J.-S.; Lee, D.-W.; Lee, D.-H.; Jeong, D.-S. Imidazole Derivatives and Organic Electronic Device Using the Same. U.S. Patent WO 2007/011163, 25 January 2007.

44. Islam, A.; Zhang, D.; Ouyang, X.; Yang, R.; Lei, T.; Hong, L.; Peng, R.; Duan, L.; Ge, Z. Multifunctional Emitters for Efficient Simplified Non-Doped Blueish Green Organic Light Emitting Devices with Extremely Low Efficiency Roll-off. *J. Mater. Chem. C* **2017**, *5*, 6527–6536. [CrossRef]

45. Sun, Y.-F.; Huang, W.; Lu, C.-G.; Cui, Y.-P. The Synthesis, Two-Photon Absorption and Blue Upconversion Fluorescence of Novel, Nitrogen-Containing Heterocyclic Chromophores. *Dye. Pigment.* **2009**, *81*, 10–17. [CrossRef]

46. Fridman, N.; Kaftory, M.; Speiser, S. Structures and Photophysics of Lophine and Double Lophine Derivatives. *Sens. Actuators B Chem.* **2007**, *126*, 107–115. [CrossRef]

47. Chang, Y.-T.; Hsu, S.-L.; Su, M.-H.; Wei, K.-H. Intramolecular Donor–Acceptor Regioregular Poly(Hexylphenanthrenyl-Imidazole Thiophene) Exhibits Enhanced Hole Mobility for Heterojunction Solar Cell Applications. *Adv. Mater.* **2009**, *21*, 2093–2097. [CrossRef]

48. Eseola, A.O.; Li, W.; Gao, R.; Zhang, M.; Hao, X.; Liang, T.; Obi-Egbedi, N.O.; Sun, W.-H. Syntheses, Structures, and Fluorescent Properties of 2-(1H-Imidazol-2-Yl)Phenols and Their Neutral Zn(II) Complexes. *Inorg. Chem.* **2009**, *48*, 9133–9146. [CrossRef] [PubMed]

49. Liu, D.; Yang, L.; Wu, Y.; Wang, X.; Zeng, Y.; Han, G.; Yao, H.; Li, S.; Zhang, S.; Zhang, Y.; et al. Tunable Electron Donating and Accepting Properties Achieved by Modulating the Steric Hindrance of Side Chains in A-D-A Small-Molecule Photovoltaic Materials. *Chem. Mater.* **2018**, *30*, 619–628. [CrossRef]

50. Chu, T.-Y.; Lu, J.; Beaupré, S.; Zhang, Y.; Pouliot, J.-R.; Zhou, J.; Najari, A.; Leclerc, M.; Tao, Y. Effects of the Molecular Weight and the Side-Chain Length on the Photovoltaic Performance of Dithienosilole/Thienopyrrolodione Copolymers. *Adv. Funct. Mater.* **2012**, *22*, 2345–2351. [CrossRef]

51. Medlej, H.; Awada, H.; Abbas, M.; Wantz, G.; Bousquet, A.; Grelet, E.; Hariri, K.; Hamieh, T.; Hiorns, R.C.; Dagron-Lartigau, C. Effect of Spacer Insertion in a Commonly Used Dithienosilole/Benzothiadiazole-Based Low Band Gap Copolymer for Polymer Solar Cells. *Eur. Polym. J.* **2013**, *49*, 4176–4188. [CrossRef]

52. Cao, D.; Liu, Q.; Zeng, W.; Han, S.; Peng, J.; Liu, S. Diketopyrrolopyrrole-Containing Polyfluorenes: Facile Method To Tune Emission Color and Improve Electron Affinity. *Macromolecules* **2006**, *39*, 8347–8355. [CrossRef]

53. Li, S.; Kang, H.; Wu, W.; Ye, C. Synthesis and Properties of a Second-Order, Nonlinear-Optical, Addition-Type Polyimide with High Thermal and Temporal Stability. *J. Appl. Polym. Sci.* **2008**, *110*, 3758–3762. [CrossRef]

54. Kulhánek, J.; Bureš, F. Imidazole as a Parent π-Conjugated Backbone in Charge-Transfer Chromophores. *Beilstein J. Org. Chem.* **2012**, *8*, 25–49. [CrossRef] [PubMed]

55. Crosby, G.A.; Demas, J.N. Measurement of Photoluminescence Quantum Yields. Review. *J. Phys. Chem.* **1971**, *75*, 991–1024. [CrossRef]

56. Dominguez, Z.; Khuong, T.-A.V.; Dang, H.; Sanrame, C.N.; Nuñez, J.E.; Garcia-Garibay, M.A. Molecular Compasses and Gyroscopes with Polar Rotors: Synthesis and Characterization of Crystalline Forms. *J. Am. Chem. Soc.* **2003**, *125*, 8827–8837. [CrossRef] [PubMed]

57. Subeesh, M.S.; Shanmugasundaram, K.; Sunesh, C.D.; Chitumalla, R.K.; Jang, J.; Choe, Y. Host–Dopant System To Generate Bright Electroluminescence from Small Organic Molecule Functionalized Light-Emitting Electrochemical Cells. *J. Phys. Chem. C* **2016**, *120*, 12207–12217. [CrossRef]

58. Levi, L.; Müller, T.J.J. Multicomponent Syntheses of Functional Chromophores. *Chem. Soc. Rev.* **2016**, *45*, 2825–2846. [CrossRef] [PubMed]

59. Xue, H.; Zhao, Y.; Wu, H.; Wang, Z.; Yang, B.; Wei, Y.; Wang, Z.; Tao, L. Multicomponent Combinatorial Polymerization via the Biginelli Reaction. *J. Am. Chem. Soc.* **2016**, *138*, 8690–8693. [CrossRef]

60. Murugesan, V.; de Bettignies, R.; Mercier, R.; Guillerez, S.; Perrin, L. Synthesis and Characterizations of Benzotriazole Based Donor–Acceptor Copolymers for Organic Photovoltaic Applications. *Synth. Met.* **2012**, *162*, 1037–1045. [CrossRef]

61. Jin, Y.; Xu, Y.; Liu, Y.; Wang, L.; Jiang, H.; Li, X.; Cao, D. Synthesis of Novel Diketopyrrolopyrrole-Based Luminophores Showing Crystallization-Induced Emission Enhancement Properties. *Dye. Pigment.* **2011**, *90*, 311–318. [CrossRef]

62. Saes, B.W.H.; Lutz, M.; Wienk, M.M.; Meskers, S.C.J.; Janssen, R.A.J. Tuning the Optical Characteristics of Diketopyrrolopyrrole Molecules in the Solid State by Alkyl Side Chains. *J. Phys. Chem. C* **2020**, *124*, 25229–25238. [CrossRef] [PubMed]

63. Berhman, I. *Energy Transfer Parameters of Aromatic Compounds*; Elsevier: Amsterdam, The Netherlands, 1973; p. 390. ISBN 9780323152570.

64. Costa, J.C.S.; Taveira, R.J.S.; Lima, C.F.R.A.C.; Mendes, A.; Santos, L.M.N.B.F. Optical Band Gaps of Organic Semiconductor Materials. *Opt. Mater. (Amst.)* **2016**, *58*, 51–60. [CrossRef]